Geometrically nonlinear analysis of composite beams using Wiener-Milenkovi# parameters

Qi Wang and Wenbin Yu

Citation: Journal of Renewable and Sustainable Energy **9**, 033306 (2017); doi: 10.1063/1.4985091
View online: http://dx.doi.org/10.1063/1.4985091
View Table of Contents: http://aip.scitation.org/toc/rse/9/3
Published by the American Institute of Physics

Geometrically nonlinear analysis of composite beams using Wiener-Milenković parameters

Qi Wang[1,a)] and Wenbin Yu[2]
[1]*Siemens Wind Power, Inc., Boulder, Colorado 80302, USA*
[2]*School of Aeronautics and Astronautics, Purdue University, West Lafayette, Indiana 47907, USA*

(Received 31 January 2017; accepted 22 May 2017; published online 7 June 2017)

This paper presents a geometrically nonlinear analysis of composite beams including static, dynamic, and eigenvalue analyses. With the increase in size and flexibility of engineering components such as wind turbine blades, geometric nonlinearity plays an increasingly significant role in structural analysis. The Geometric Exact Beam Theory (GEBT), pioneered by Reissner and extended by Hodges, is adopted as the foundation for this work. Special emphasis is placed on the vectorial parameterization of finite rotation, which is a fundamental aspect in the geometrically nonlinear formulation. This method is introduced based on Euler's rotation theorem and the property of rotation operation: the length preservation of the rotated vector. The GEBT is then implemented with the Wiener-Milenković parameters using a mixed formulation. Several numerical examples are studied based on the derived theory, and the results are compared with analytical solutions and those available in the literature. The analysis of a realistic composite wind turbine blade is provided to show the capability of the present model for generalized composite slender structures. It concludes that the proposed model can be used as a beam tool in a multibody framework whose valid range of rotation is up to 2π. *Published by AIP Publishing.* [http://dx.doi.org/10.1063/1.4985091]

I. INTRODUCTION

Many engineering components that have one of their dimensions larger than the other two can be idealized as beams, e.g., bridges in civil engineering, joists, and lever arms in heavy machine industries and helicopter rotor blades in aeronautics. This work[1] is motivated by the need for higher fidelity numerical models for the structural design of modern composite wind turbine blades. In weight-critical applications of beam structures, such as wings in aerospace and blades in wind energy, composite materials are attractive due to their superior weight-to-strength and weight-to-stiffness ratios. However, the use of composites complicates engineering analysis because of the coupling effects in the structure. Moreover, geometric nonlinearity is crucial to the analysis of highly flexible composite beam structures, especially when applied to unprecedented-length turbine blades.[2] The term "geometrically exact" suggests that there is no approximation invoked in defining beam strains in terms of large displacements and rotations in the theory.

The intrinsic formulation of the geometrically exact beam theory was first proposed by Reissner[3] in 1973. Here, the "intrinsic formulation" indicates that the one-dimensional (1D) beam strains are developed in terms of virtual displacement and virtual rotation quantities so that the formulation is not tied to a specific choice of displacement or rotation variables.[4] Simo[5] and Simo and Vu-Quoc[6] extended Reissner's work to handle three-dimensional (3D) dynamic problems. Since then, researchers have been reporting many extensions and applications of geometric exact beam theory (GEBT), where significant efforts have been invested in dealing with finite

Note: Presented at the 54th AIAA/ASME/ASCE/AHS/ASC Structures, Structural Dynamics, and Materials Conference, Boston, Massachusetts, 8–11 April 2013.

[a)]Electronic mail: aaron.qi.wang@gmail.com

rotations. Jelenić and Crisfield[7] implemented this theory based on the finite element method where a new approach for interpolating the rotation field was introduced to preserve the geometric exactness. Betsch and Steinmann[8] circumvented the interpolation of rotation by introducing a reparameterization of the weak form corresponding to the equations of motion of GEBT. It is noted that Ibrahimbegović[9] implemented this theory by considering the initial twist and curvatures. More details on the vector-like parameterization of 3D finite rotations of this work were presented in Ref. 10. Ibrahimbegović and Mikdad[11] then extended the previous static implementation to include dynamics. A brief review on the geometrically exact beam theory and its implementation can be found in Ref. 12. In contrast to the displacement-based implementations, the geometrically exact beam theory has also been formulated by mixed finite elements where both the primary and dual fields are independently interpolated.[13] In the mixed formulation, all the necessary ingredients including Hamilton's principle and the kinematic equations are combined in a single variational formulation statement with Lagrange multipliers, and the motion variables, generalized strains, forces and moments, linear and angular momenta, and displacement and rotation variables are considered as independent quantities. Yu and Blair[14] presented the implementation of GEBT in a mixed formulation where Rodrigues parameters are chosen to represent the finite rotation. In that work, a new time-marching scheme was proposed, which is more efficient than the one developed by Patil *et al.*[15] Yu and Blair's work resulted in an open source general-purpose composite beam solver called "GEBT." The readers are referred to a textbook by Hodges,[4] where comprehensive derivations and discussions on nonlinear composite beam theories can be found. It is noted that these beam tools such as GEBT need a cross-sectional analysis as pre-processing to provide the stiffness constants. For composite materials, all the elastic couplings among extension, bending, shear, and torsion exist so that high-fidelity cross-sectional tools are needed, including VABS[16,17] and BECAS.[18]

The objectives of this paper are as follows: (1) to implement a geometric exact beam theory with a Wiener-Milenković parameter based on the work by Yu and Blair[14] and (2) to demonstrate the application of this approach in the analysis of composite beams. It is shown that GEBT has great potential for fluid-structure interaction studies along with other fluid theories. For example, Li *et al.*[19] presented an innovative and efficient approach by combining GEBT and discrete vortex method (DVM) together in a tidal turbine analysis, which has the same accuracy level as the three-dimensional finite element solution but much less computational cost. The authors expect that this paper will clear the path for a wider and easier use of GEBT in modern wind turbine structural design and analysis. The outline of this paper is as follows: In Sec. II, we recapitulate Euler's rotation theorem and the rotation tensor and introduce the concept of vectorial parameterization of finite rotation. The equations of the geometrically exact beam theory and the mixed formulation using Wiener-Milenković parameters are discussed in Sec. III. In Sec. IV, we present a number of numerical examples including static, dynamic, and eigenvalue analyses of isotropic and composite beams, which validate the present theory and illustrate the capability of this beam solver. Conclusions are provided in Sec. V.

II. VECTORIAL PARAMETERIZATION OF ROTATION

This section reviews the theories of the rotation tensor and vectorial parameterization for completeness of this paper. The content of this section can be found in many other papers and textbooks.

A. Euler's rotation theorem and rotation tensor

Euler's rotation theorem states that an arbitrary motion of a rigid body that leaves one of its points fixed can be represented by a single rotation of magnitude ϕ about unit vector $\bar{n}$.[20] Figure 1 shows the configuration of the problem where vector $\underline{a}$ rotates magnitude ϕ about unit vector $\bar{n}$, and the new vector after rotation is denoted as $\underline{b}$. In our adopted notation, $\overline{(\cdot)}$ denotes a unit vector, while a single underline and double underlines denote a vector and a tensor, respectively. These two vectors are related as

$$\underline{b} = \underline{\underline{C}}^T \underline{a}, \tag{1}$$

where $\underline{\underline{C}}$ is the rotation tensor and the superscript T denotes the transpose. The fundamental property of a rotation operation is to preserve the length; the vector length does not change when computed from its components resolved in different arbitrary orthonormal bases. For example, $\|\underline{a}\| = \|\underline{b}\|$, where $\|\cdot\|$ denotes the Euclidean vector norm, which leads to

$$\bar{n}^T \underline{a} = \|\underline{a}\| \cos\alpha = \|\underline{b}\| \cos\alpha, \tag{2}$$

$$\|\tilde{n}\underline{a}\| = \|\underline{a}\| \sin\alpha = \|\underline{b}\| \sin\alpha. \tag{3}$$

The tilde operator $(\tilde{\cdot})$ defines a second-order, skew-symmetric tensor corresponding to the given vector. In the literature, it is also termed as the "cross-product matrix." For example,

$$\tilde{n} = \begin{bmatrix} 0 & -n_3 & n_2 \\ n_3 & 0 & -n_1 \\ -n_2 & n_1 & 0 \end{bmatrix}.$$

The following equations can be drawn from the geometry depicted in Fig. 1:

$$\underline{b} = \underline{OC} + \underline{CB} = \|\underline{b}\| \cos\alpha\, \bar{n} + \|\underline{b}\| \sin\alpha [\bar{s}\cos\phi + \bar{t}\sin\phi]. \tag{4}$$

Unit vector $\bar{t}$ is along the vector product of vectors $\bar{n}$ and $\underline{a}$

$$\bar{t} = \frac{\tilde{n}\underline{a}}{\|\tilde{n}\underline{a}\|} \tag{5}$$

and unit vector $\bar{s}$ is

$$\bar{s} = \tilde{t}\,\bar{n} = \frac{\widetilde{(\tilde{n}\underline{a})}\bar{n}}{\|\tilde{n}\underline{a}\|}. \tag{6}$$

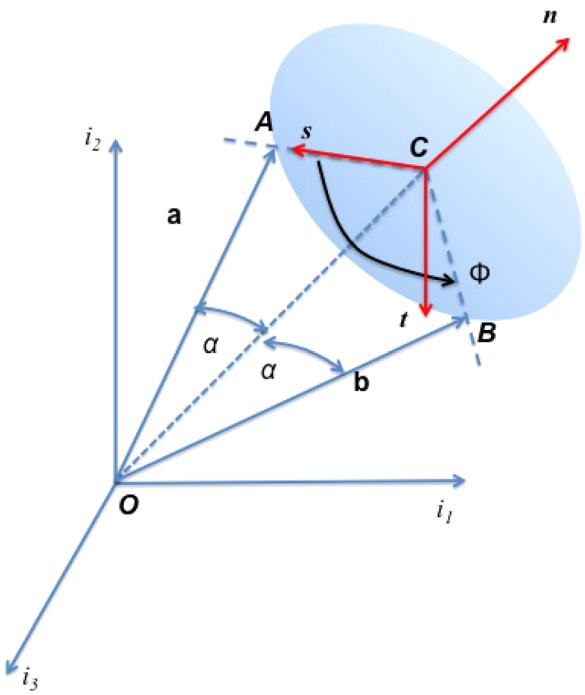

FIG. 1. A finite rotation of magnitude ϕ about **n**.

With the help of Eqs. (2), (3), (5), and (6), Eq. (4) can be written as

$$\underline{b} = \underline{a} + \sin\phi(\tilde{n}\underline{a}) + (1 - \cos\phi)\tilde{n}\tilde{n}\underline{a} = \underline{\underline{C}}^T\,\underline{a}, \tag{7}$$

where the rotation tensor $\underline{\underline{C}}$ is

$$\underline{\underline{C}} = \underline{\underline{\Delta}} - \sin\phi\,\tilde{n} + (1 - \cos\phi)\tilde{n}\tilde{n} \tag{8}$$

with $\underline{\underline{\Delta}}$ a 3×3 identity matrix. This equation is known as the Rodrigues rotation formula.

B. Wiener-Milenković parameters

A finite rotation in 3D space discussed in the previous section (Sec. II A) leads to a one-to-one vector transformation,[21] although four parameters (rotation magnitude ϕ and rotation axis $\bar{n} = \{n_1, n_2, n_3\}^T$) are used instead of three. To eliminate the redundancy in the four-parameter description and to exploit the tensorial nature of rotation, we introduce the following definition

$$\underline{c} = p(\phi)\,\bar{n}, \tag{9}$$

where $\underline{c}$ is the rotation parameter vector and $p(\phi)$ is the generating function. For the Wiener-Milenković parameters used in the present paper,

$$p(\phi) = 4\tan\frac{\phi}{4}. \tag{10}$$

A singularity can be observed in this representation since $\|\underline{c}\| \to \infty$ when $|\phi| \to 2\pi$.

Substituting Eq. (9) into (8), the explicit expression of the rotation tensor in terms of the vectorial parameterization can be obtained as

$$\underline{\underline{C}} = \underline{\underline{\Delta}} - \frac{\sin\phi}{p(\phi)}\tilde{c} + \frac{1 - \cos\phi}{p^2(\phi)}\tilde{c}\tilde{c}. \tag{11}$$

For the Wiener-Milenković parameters, the rotation tensor is found by substituting Eq. (10) into Eq. (11) as

$$\underline{\underline{C}}(\underline{c}) = \frac{1}{(4 - c_0)^2}\left[(c_0^2 - \underline{c}^T\underline{c})\underline{\underline{\Delta}} - 2c_0\tilde{c} + 2\underline{c}\underline{c}^T\right], \tag{12}$$

where c_0 is a scalar parameter defined as

$$c_0 = 2\left(1 - \tan^2\frac{\phi}{4}\right) = 2 - \frac{\underline{c}^T\underline{c}}{8}. \tag{13}$$

In the expanded form,

$$\underline{\underline{C}}(\underline{c}) = \frac{1}{(4 - c_0)^2}\begin{bmatrix} c_0^2 + c_1^2 - c_2^2 - c_3^2 & 2(c_1c_2 + c_0c_3) & 2(c_1c_3 - c_0c_2) \\ 2(c_1c_2 - c_0c_3) & c_0^2 - c_1^2 + c_2^2 - c_3^2 & 2(c_2c_3 + c_0c_1) \\ 2(c_1c_3 + c_0c_2) & 2(c_2c_3 - c_0c_1) & c_0^2 - c_1^2 - c_2^2 + c_3^2 \end{bmatrix}, \tag{14}$$

where c_1, c_2, and c_3 are the components of vector $\underline{c}$. For a linear theory, c_i values are assumed to be small, and their powers and products are negligible. The rotation matrix then reduces to

$$\underline{\underline{C}}(\underline{c}) = \underline{\underline{\Delta}} - \tilde{c}. \tag{15}$$

Interested readers are referred to a recent textbook[20] containing many aspects of multibody analysis for more details on the vectorial parameterization of finite rotations.

III. MIXED FORMULATION OF THE GEOMETRICALLY EXACT BEAM THEORY

In this section, we derive the equations used in a mixed formulation of GEBT where finite rotation is represented by the Wiener-Milenković parameters. Figure 2 shows a beam in its undeformed and deformed states. A reference frame $\mathbf{b}_i$ is introduced along the beam axis for the undeformed state; a frame $\mathbf{B}_i$ is introduced along each point of the deformed beam axis. The variational statement of the geometric exact beam theory is[4]

$$\int_{t_1}^{t_2}\int_0^l \left[\delta V^T P + \delta\Omega^T H - \delta\gamma^T F - \delta\kappa^T M + \overline{\delta q}^T f + \overline{\delta\psi}^T m\right] dx_1 dt$$
$$= \int_0^l (\overline{\delta q}^T \hat{P} + \overline{\delta\psi}^T \hat{H})|_{t_1}^{t_2} dx_1 - \int_{t_1}^{t_2} (\overline{\delta q}^T \hat{F} + \overline{\delta\psi}^T \hat{M})|_0^l dt, \tag{16}$$

where $\overline{\delta q}$ and $\overline{\delta\psi}$ are the virtual displacement and rotation, respectively; F and M are the sectional force resultant and moment resultant, respectively; P and H are the sectional linear momentum and angular momentum, respectively; V and Ω are the linear and angular velocities of the beam reference line, respectively; γ and κ are the force-strain measures and moment-strain measures, respectively; f and m are the distributed forces and moments per unit length, respectively; $\hat{F}$ and $\hat{M}$ are the forces and moments, respectively, evaluated at the ends of the space interval; and $\hat{P}$ and $\hat{H}$ are the linear momentum and angular momentum, respectively, evaluated at the ends of the time interval. It is noted that unlike in the previous section (Sec. II), the overbarred virtual quantities, $\overline{\delta(\cdot)}$, denote that the virtual quantity is not necessarily the variation of a real function in this section. Using the 1D virtual kinematic relations[4] and integrating this equation by parts with respect to t and x_1, we obtain the following:

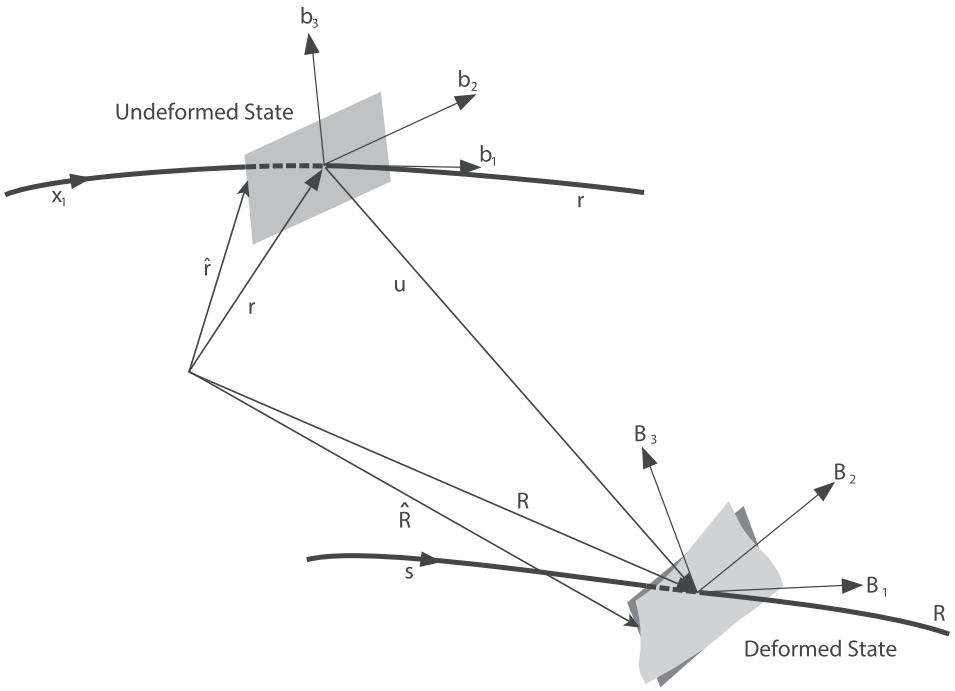

FIG. 2. Schematic showing undeformed and deformed beam configurations.[22]

$$\int_{t_1}^{t_2}\int_0^l \Big\{\overline{\delta q}^T(F' + \tilde{K}F - \dot{P} - \tilde{\Omega}P + f) + \overline{\delta\psi}^T\left[M' + \tilde{K}M + (\tilde{e}_1 + \tilde{\gamma})F - \tilde{V}P - \dot{H} - \tilde{\Omega}H + m\right]\Big\}dx_1 dt = \int_0^l \left[\overline{\delta q}^T\check{P} + \overline{\delta\psi}^T\check{H}\right]\Big|_{t_1}^{t_2} dx_1 - \int_{t_1}^{t_2}\left[\overline{\delta q}^T\check{F} + \overline{\delta\psi}^T\check{M}\right]\Big|_0^l dt, \tag{17}$$

where $K = \kappa + k$ is the summation of moment-strain measures and initial curvatures; e_1 is defined as a column matrix as $e_1 = \lfloor 1\ 0\ 0 \rfloor^T$. The check operator on the right-hand-side of the equation is defined as $(\check{\cdot}) = (\hat{\cdot}) - (\cdot)$. The "primed" and "dotted" terms represent their spatial and temporal partial derivatives, respectively. Note that all the quantities in Eqs. (16) and (17) are expressed in the deformed base $\underline{B}$. The constitutive equations relate the velocities to the momenta and the 1D strain measures to the sectional resultants as

$$\begin{Bmatrix} P \\ H \end{Bmatrix} = I \begin{Bmatrix} V \\ \Omega \end{Bmatrix}, \tag{18}$$

$$\begin{Bmatrix} F \\ M \end{Bmatrix} = S \begin{Bmatrix} \gamma \\ \kappa \end{Bmatrix}, \tag{19}$$

where I and S are the sectional mass and stiffness matrices, respectively. For composite beam structures, the sectional stiffness matrix S could be fully populated, which means that all of the fundamental deformation modes, including extension, shear, torsion, and bending, could be coupled.

To derive the mixed formulation, we need to incorporate the kinematical relations into the original variational statement of Hamilton's principle to obtain a new functional so that all the variables can vary independently in the calculus of variations. The 1D kinematical equations are written as

$$u' = C^{bB}(e_1 + \gamma) - e_1 - \tilde{k}u, \tag{20}$$

$$\dot{u} = C^{bB}V - v - \tilde{\omega}u, \tag{21}$$

$$c' = Q^{-1}(\kappa + k - C^{Bb}k), \tag{22}$$

$$\dot{c} = Q^{-1}(\Omega - C^{Bb})\omega, \tag{23}$$

where u is the 1D displacement; C^{Bb} is the rotation matrix and $C^{Bb} = (C^{bB})^T$; v and ω are the linear and angular velocities of undeformed triad $\mathbf{b}$ in the inertial frame; c are the Wiener-Milenković parameters introduced in the previous section (Sec. II); and Q is a matrix defined as

$$Q = \frac{1}{(4 - c_0)^2}\left[\left(4 - \frac{1}{4}c^T c\right)\Delta - 2\tilde{c} + \frac{1}{2}cc^T\right] \tag{24}$$

and

$$Q^{-1} = \left(1 - \frac{1}{16}c^T c\right)\Delta + \frac{1}{2}\tilde{c} + \frac{1}{8}cc^T. \tag{25}$$

Interested readers are referred to Ref. 4 for the detailed derivation of Eqs. (20)–(23). These kinematical equations are adjoined to Eq. (16) by Lagrange multipliers so that the left-hand-side becomes

$$\int_{t_1}^{t_2}\int_0^l \Big\{\delta V^T P + \delta\Omega^T H - \delta\gamma^T F - \delta\kappa^T M + \overline{\delta q}^T f + \overline{\delta\psi}^T m + \delta\big[\lambda_1(u' - C^{bB}(e_1+\gamma) + e_1 + \tilde{k}u)\big] + \delta\big[\lambda_2(\dot{u} - C^{bB}V + v + \tilde{\omega}u)\big] + \delta\big[\lambda_3(c' - Q^{-1}(\kappa + k - C^{Bb}k)u)\big] + \delta\big[\lambda_4(\dot{c} - Q^{-1}(\Omega - C^{Bb}))\big]\Big\}dx_1 dt. \tag{26}$$

The Lagrange multipliers, λ_i, can be identified by using the condition that virtual quantities can be independently and arbitrarily varied. For example, for the virtual strain $\delta\gamma$ to be arbitrary, the following equation needs to be satisfied:

$$-F - C^{Bb}\lambda_1^T = 0. \tag{27}$$

Hence, the value of λ_1 can be expressed as $\lambda_1^T = -C^{bB}F$.

To deal with moving beams, we introduce a global body-attached coordinate system $\underline{a}$, and it is clear that the relation C^{ab} between frame a and undeformed frame b is determined and time independent. If we introduce another set of Wiener-Milenković parameters c_a which is defined in frame a, then the following equation can be derived:

$$C^{Ba} = C^{ba}C, \tag{28}$$

with C a function of c_a identical to C^{Bb} in Eq. (14) where c is replaced by c_a. After identifying the Lagrange multipliers in Eq. (26), the variational statement in Eq. (17) can be rewritten as

$$\begin{aligned}\int_0^l \Big\{&\delta u_a'^T F_a + \overline{\delta\psi}_a'^T M_a + \delta u_a^T(\dot{P}_a + \tilde{\omega}_a P_a) \\ &+ \overline{\delta\psi}_a^T\big[\dot{H}_a + \tilde{\omega}_a H_a + \tilde{V}_a P_a - C^{aB}(\tilde{e}_1 + \tilde{\gamma})F_B\big] \\ &- \overline{\delta F}_a^T\big[C^{aB}(e_1+\gamma) - C^{ab}e_1\big] - \overline{\delta F}_a'^T u_a - \overline{\delta M}_a'^T c_a \\ &- \overline{\delta M}_a^T Q_a^{-1}C^{ab}\kappa + \overline{\delta P}_a^T(V_a - v_a - \tilde{\omega}_a u_a - \dot{u}_a) \\ &+ \overline{\delta H}_a^T(\Omega_B - \omega_B - C^{ba}Q_a\dot{c}_a) - \delta u_a^T f_a - \overline{\delta\psi}_a^T m_a\Big\}dx_1 \\ &= (\delta u_a^T\hat{F}_a + \overline{\delta\psi}_a^T\hat{M}_a - \overline{\delta F}_a^T\hat{u}_a - \overline{\delta M}_a^T\hat{c}_a)\big|_0^l.\end{aligned} \tag{29}$$

It is pointed out that the time derivatives of virtual quantities are removed by carrying out integration by parts, and Q_a is defined similar to Eq. (28) as

$$Q_a = C^{ab}QC^{ba}. \tag{30}$$

The subscripts in Eq. (29) indicate in which frame the quantities are defined, and they can be easily transformed between different frames using the rotation matrix.

Equation (29) contains all the information needed for the mixed formulation of the geometric exact beam theory. We consider u_a, c_a, F_B, M_B, P_B, and H_B as the fundamental unknown variables. Linear shape functions are used for test functions δu_a, $\overline{\delta\psi}_a$, $\overline{\delta F}_a$, and $\overline{\delta M}_a$ since only the first order spatial derivatives appear in these terms and constant shape functions are used for $\overline{\delta P}_a$ and $\overline{\delta H}_a$.

Dividing a beam into N elements with the starting node of the i element numbered as i and the ending number as $i+1$, and using the linear and constant shape functions for different variables, the integration in Eq. (29) can be calculated analytically. Finally, we conclude the following finite element equations:

$$f_{u_1}^- - F_1^* = 0, \tag{31}$$

$$f_{\psi_1}^- - M_1^* = 0, \tag{32}$$

$$f_{F_1}^- - \hat{u}_1 = 0, \tag{33}$$

$$f_{M_1}^- - \hat{c}_1 = 0 \tag{34}$$

at the starting node and

$$f_{u_N}^+ - F_{N+1}^* = 0, \tag{35}$$

$$f_{\psi_N}^+ - M_{N+1}^* = 0, \tag{36}$$

$$f_{F_N}^+ + \hat{u}_{N+1} = 0, \tag{37}$$

$$f_{M_N}^+ + \hat{c}_{N+1} = 0 \tag{38}$$

at the ending node. Note that F_1^*, M_1^*, F_{N+1}^*, and M_{N+1}^* are the external forces/moments balancing the internal resultants. At each intermediate point, the equations are

$$f_{u_i}^+ + f_{u_{i+1}}^- = 0, \tag{39}$$

$$f_{\psi_i}^+ + f_{\psi_{i+1}}^- = 0, \tag{40}$$

$$f_{F_i}^+ + f_{F_{i+1}}^- = 0, \tag{41}$$

$$f_{M_i}^+ + f_{M_{i+1}}^- = 0, \tag{42}$$

where $i = 1, 2\ldots, N-1$. Also, for each element, we have

$$f_{P_i} = 0, \tag{43}$$

$$f_{H_i} = 0, \tag{44}$$

where $i = 1,\ldots, N$. The f matrices in the above equations are calculated analytically from the integration in Eq. (29) and written as

$$f_{u_i}^{\mp} = \mp C^T C^{ab} F_i - \bar{f}_i^{\mp} + \frac{\Delta L_i}{2}\left[\tilde{\omega}_a C^T C^{ab} P_i + \overline{\dot{C^T C^{ab}} P_i}\right], \tag{45}$$

$$f_{\psi_i}^{\mp} = \mp C^T C^{ab} M_i - \bar{m}_i^{\mp} + \frac{\Delta L_i}{2}\left[\tilde{\omega}_a C^T C^{ab} H_i + \overline{\dot{C^T C^{ab}} H_i} + C^T C^{ab}(\tilde{V}_i P_i - (\tilde{e}_1 + \tilde{\gamma}_i) F_i)\right], \tag{46}$$

$$f_{F_i}^{\mp} = \pm u_i - \frac{\Delta L_i}{2}\left[C^T C^{ab}(e_1 + \gamma_i) - C^{ab} e_1\right], \tag{47}$$

$$f_{M_i}^{\mp} = \pm c_i - \frac{\Delta L_i}{2} Q_a^{-1} C^{ab} \kappa_i, \tag{48}$$

$$f_{P_i} = C^T C^{ab} V_i - v_i - \tilde{\omega}_a u_i - \dot{u}_i, \tag{49}$$

$$f_{H_i} = \Omega_i - C^{ba} C \omega_a - C_{ba} Q_a \dot{c}_i, \tag{50}$$

with

$$\bar{f}_i^- = \int_0^1 (1-\eta) f_a \Delta L_i d\eta, \tag{51}$$

$$\bar{f}_i^+ = \int_0^1 \eta f_a \Delta L_i d\eta, \tag{52}$$

$$\bar{m}_i^- = \int_0^1 (1-\eta) m_a \Delta L_i d\eta, \tag{53}$$

$$\bar{m}_i^+ = \int_0^1 \eta m_a \Delta L_i d\eta, \tag{54}$$

where ΔL_i is the length of the ith element; L_i is the x_1 coordinate of the starting node; and η is a general coordinate defined as

$$\eta = \frac{x_1 - L_i}{\Delta L_i}. \tag{55}$$

In the governing equations from Eqs. (31) to (44), those corresponding to f_u and f_ψ are the equations of motion; the equations corresponding to f_F and f_M are the strain-displacement equations; and the equations corresponding to f_P and f_H are the velocity-displacement kinematical equations. These equations can also be written in the symbolic form as

$$\mathcal{F}(X, \dot{X}) = 0, \tag{56}$$

where $\mathcal{F}$ is a system of $18N + 6M$ equations and X is a vector containing $18N + 6M$ unknowns. Here, N is the number of elements and M is the total number of boundary points and connection points in beam or beam assemblies.

The system of nonlinear equations is solved using the Newton-Raphson method along with line search to guarantee global convergence. A Newmark type time marching scheme is derived for transient analysis. For the eigenvalue analysis, GEBT calculates the steady state solution first, and the eigenvalue analysis is performed corresponding to this state. The readers are referred to Yu and Blair[14] for more details on eigenvalue solvers and time marching schemes in solving these equations.

IV. NUMERICAL EXAMPLES

A. Example 1: Static bending of a cantilever beam

The first example is a benchmark problem for the geometrically nonlinear analysis of beams.[5,23] We calculate the static deflection of a cantilever beam that is subjected at its free end to a constant moment M. The length of the beam L is 12 in., and the side length of the square section is 1 in. The beam is discretized into 16 elements in the GEBT calculation. The Young's modulus E of the material is given as 30×10^6 lb/in^4. The moment applied to the beam is $M = \lambda \bar{M}$, where $\bar{M} = \pi \frac{EI}{L}$. The parameter λ will vary between 0 and 2. Here, the tip displacements are compared with the analytical solutions, which can be found in the study by Mayo *et al.*[24] Table I lists the analytical solution and the results obtained by the current GEBT calculation. A very tight convergence tolerance of 1.0×10^{-12} for the residual value in the Newton-Raphson algorithm has been applied to all the numerical examples. Good agreement between these two sets of results is observed. It is noted that as the applied moment is increased, the number of iterations needed to obtain converged results in GEBT increases, and a singularity exists when the rotation angle reaches 2π. The GEBT result is approximated by given λ as 1.96 (see the last line in Table I). The deformation of the beam under different applied bending momenta is presented in Fig. 3. The results obtained by the original version of GEBT using Rodrigues parameters, denoted as GEBT (Rodrigues), are also listed in Table I. It can be observed that by using Rodrigues rotation parameters, the singularity is observed when the rotation reaches π.

TABLE I. Tip displacements of the cantilever beam subject to a constant moment (in inches).

λ	Analytical solution	GEBT	Iteration number	GEBT (Rodrigues)	Iteration number (Rodrigues)
0.4	[−2.9181, 6.5984]	[−2.9161, 6.6004]	9	[−2.9175, 6.6016]	9
0.8	[−9.1935, 8.6374]	[−9.1946, 8.6455]	14	[−9.2220, 8.6333]	15
1.0	[−12.0000, 7.6394]	[−12.0062, 7.6466]	14	[−12.0848, 7.6239]	1329
1.2	[−13.8710, 5.7583]	[−13.8800, 5.7576]	19	…	…
1.6	[−14.2705, 1.6496]	[−14.2403, 1.6287]	25	…	…
2.0	[−12.0, 0.0]	[−11.9017, −0.0709]	968	…	…

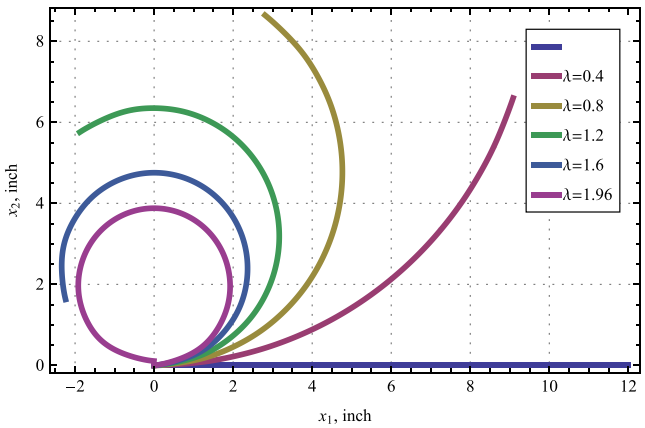

FIG. 3. Calculated deformation of a cantilever beam of example 1 under several constant bending moments.

B. Example 2: Static bending of a curved beam in 3D space

The second example is to validate the capability of GEBT for initially curved beams. We calculate the static deflection of a 45°-bend cantilever beam subjected to a concentrated end load, which was proposed by Bathe and Bolourchi[25] and is widely used as a benchmark for curved-beam analysis. The beam lies in the x–y plane, while the tip load is applied along the z direction with the magnitude $P = 600$ lb. The radius of curvature is 100 in., and the material properties are given as $E = 10^7$ psi and $\nu = 0.0$. The side length of the square cross-section of the beam is 1.0 in. A sketch of the problem is presented in Fig. 4. In the GEBT calculation, the

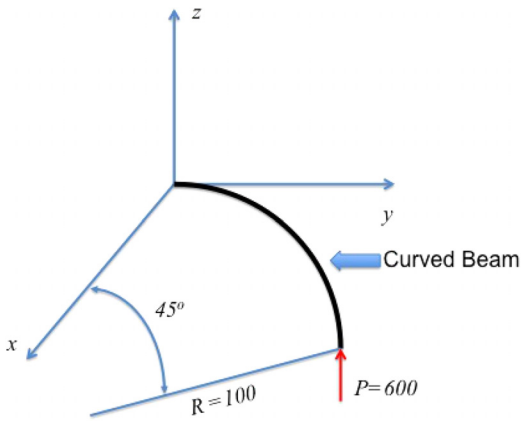

FIG. 4. Schematic of the undeformed curved beam used in example 2.

TABLE II. Tip displacements of a curved beam subject to a concentrated load (in inches).

	Bathe-Bolourchi[25]	GEBT
U_1	−13.4	−13.4
U_2	−23.5	−23.5
U_3	53.4	53.4

beam is discretized as 16 elements. The tip displacements are provided in Table II for comparison, and good agreement is demonstrated.

C. Example 3: Dynamic analysis of a beam assembly

The capability of analyzing beam assemblies and dynamic behavior of GEBT is tested in this example. A joined-beam model with two cantilever beam members meeting at their tips is used for the analysis.[26] The sketch of this beam assembly is presented in Fig. 5, and the cross-section of the cantilever is rectangular with a width of 0.1 m and a thickness of 0.05 m. The material properties of the beam are given as follows: $E = 70\,\text{GPa}$, $\nu = 0.35$, and $\rho = 2700\,\text{kg/m}^3$. A sinusoidal vertical force is applied at the joint of the beam assembly, which is given by

$$F_z(t) = \begin{cases} 0 & t < 0 \\ A_F \sin(\omega_F t) & t \geq 0, \end{cases} \tag{57}$$

with $A_F = 1.0 \times 10^5\,\text{N}$ and $\omega_F = 20\,\text{rad/s}$. Each beam member is discretized into 10 elements. The results obtained by GEBT are compared with those from an ANSYS calculation. BEAM 188 elements are used, and the mesh is the same as that used in GEBT. The time step is 0.001 s in GEBT and ANSYS. The non-zero displacement components of the joint are plotted in Fig. 6, and a good agreement is shown. Since the rotations are described by the rotation parameters in the present work, it is easy to deal with another important case in structural analysis, the structure with a follower force. Let $\underline{F}_1^b$ denote the load vector applied to the structure before deformation and resolved in the $\underline{b}_i$ frame. It can be written in the body-attached $\underline{a}_i$ frame as $\underline{F}_1^b = \underline{\underline{C}}^{ba}\underline{F}^a$. In the deformed configuration, the load vector is written as $\underline{F}_2^B$ with superscript in the frame in which the quantity is resolved. Given that it is a follower force, the components of vector $\underline{F}_2^B$ are equal to $\underline{F}_1^b$, i.e., $\underline{F}_2^B = \underline{F}_1^b$. Therefore, the load vector in the deformation

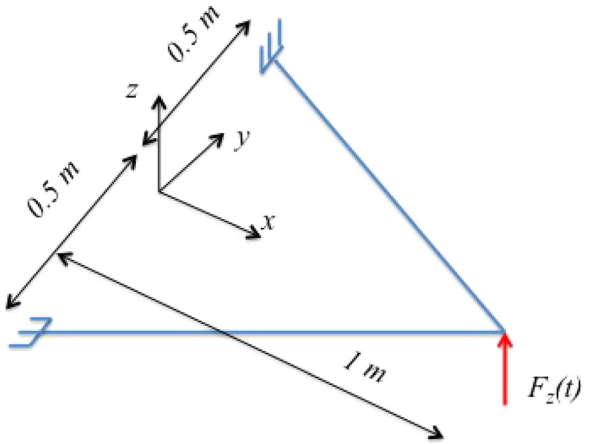

FIG. 5. Schematic of the undeformed joint beam assembly used in example 3.

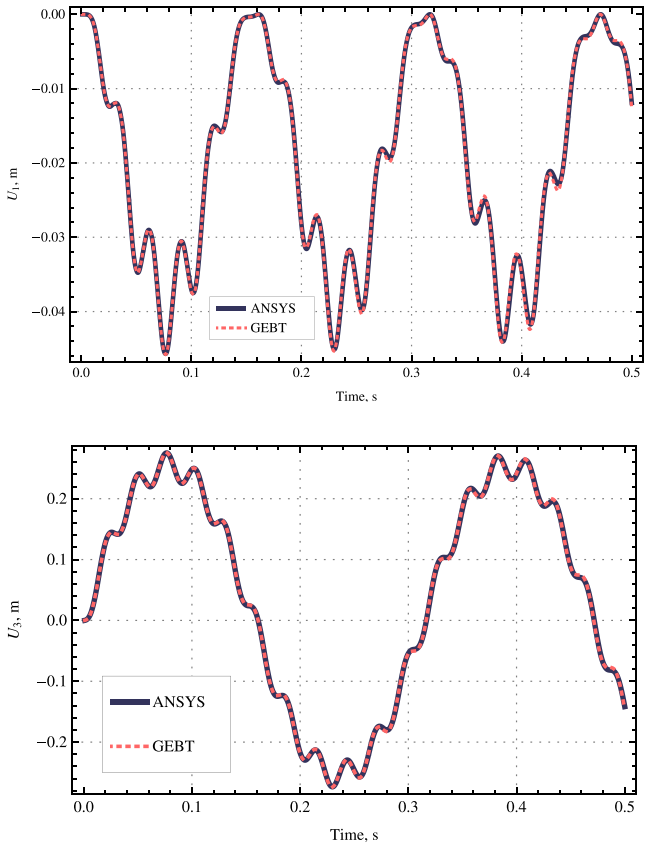

FIG. 6. ANSYS and GEBT calculated tip displacement histories of the joined beam under a vertical tip load.

resolved in the body-attached frame is derived as $\underline{F}_a = \underline{\underline{C}}^{aB}\underline{F}_2^B = \underline{\underline{C}}^{aB}\underline{\underline{C}}^{ba}\underline{F}^a = \underline{\underline{C}}^T\underline{F}^a$, where $\underline{\underline{C}}$ is the rotation tensor in the $\underline{a}_i$ frame defined in Eq. (28). Figure 7 shows the behavior of this beam assembly under a dead force and a follower force. One can observe that the structure with a follower force is softer than with a dead force for nonlinear analysis.

Finally, an eigenvalue analysis was conducted using GEBT and ANSYS for validation. The lowest five natural frequencies are listed in Table III. The percent differences between the results are calculated as $\frac{\|GEBT-ANSYS\|}{ANSYS} \times 100$. Again, good agreement between the results obtained by GEBT and ANSYS is demonstrated, where the largest error is only 1.57%.

D. Example 4: Dynamic analysis of a wind turbine blade

The last example is a transient analysis of a composite beam with the cross-section that is representative of a wind turbine blade, although it is constant along the length here. An MH 104 airfoil, which was studied by Chen *et al.*,[27] is used in this case. The blade is 60 m long and cantilevered at one end. The sectional properties can be found in the study by Chen *et al.*[27] and are given as

$$I = \begin{bmatrix} 258.053 & 0.00 & 0.00 & 0.00 & 7.07839 & -71.6871 \\ & 258.053 & 0.00 & -7.07839 & 0.00 & 0.00 \\ & & 258.053 & 71.6871 & 0.00 & 0.00 \\ & & & 48.59 & 0.00 & 0.00 \\ & & \text{Symmetry} & & 2.172 & 0.00 \\ & & & & & 46.418 \end{bmatrix}, \tag{58}$$

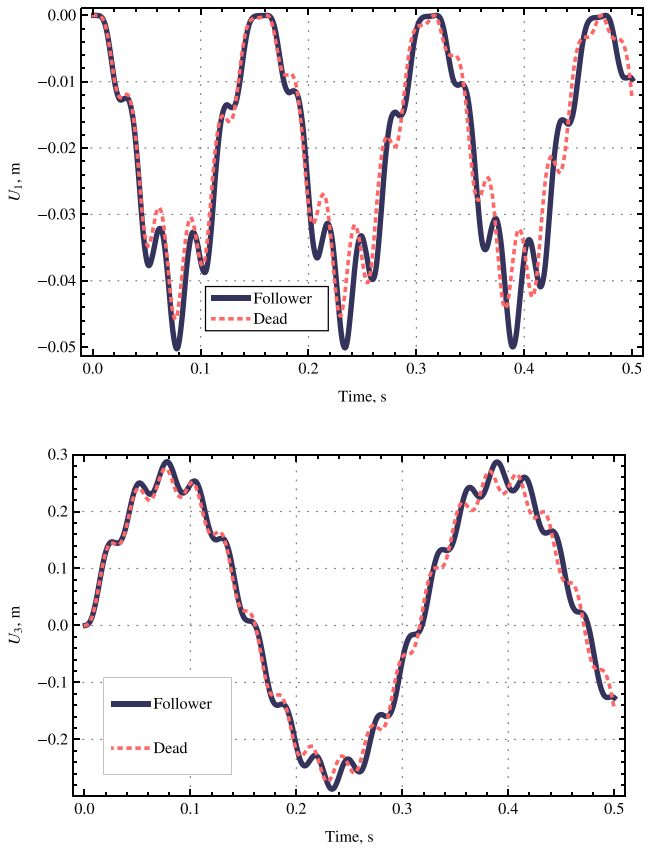

FIG. 7. ANSYS and GEBT calculated tip displacement histories of the joined beam under dead and follower vertical tip loads.

TABLE III. Comparison of natural frequencies of the beam assembly in example 3 (in Hz).

	1	2	3	4	5
GEBT	35.23	171.02	215.87	275.05	407.2
ANSYS	35.17	169.83	212.53	273.34	403.53
Percent difference	0.17	0.70	1.57	0.63	0.91

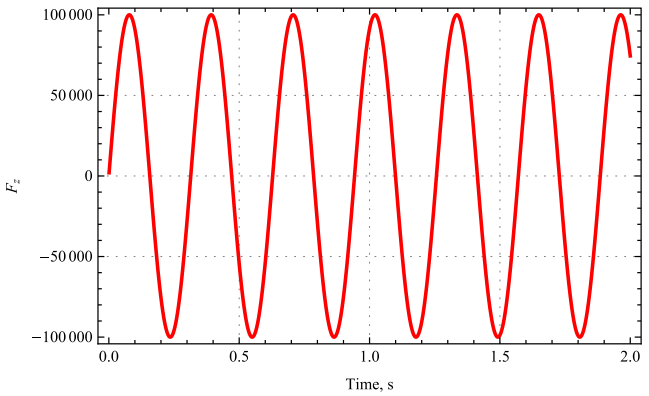

FIG. 8. The sinusoidal vertical force in example 4.

FIG. 9. Schematic of the composite wind turbine blade under vertical force in example 4.

$$S = \begin{bmatrix} 2.389\times10^{9} & 1.524\times10^{6} & 6.734\times10^{6} & -3.382\times10^{7} & -2.627\times10^{7} & -4.736\times10^{8} \\ & 4.334\times10^{8} & -3.741\times10^{6} & -2.935\times10^{5} & 1.527\times10^{7} & 3.835\times10^{5} \\ & & 2.743\times10^{7} & -4.592\times10^{4} & -6.869\times10^{4} & -4.742\times10^{6} \\ & & & 2.167\times10^{7} & -6.279\times10^{4} & 1.430\times10^{6} \\ & & \text{Symmetry} & & 1.970\times10^{7} & 1.209\times10^{7} \\ & & & & & 4.406\times10^{8} \end{bmatrix}. \tag{59}$$

Note that the sectional stiffness matrix is fully populated in this case, which means that full elastic coupling among extension, shear, twist, and bending is taken into consideration. The

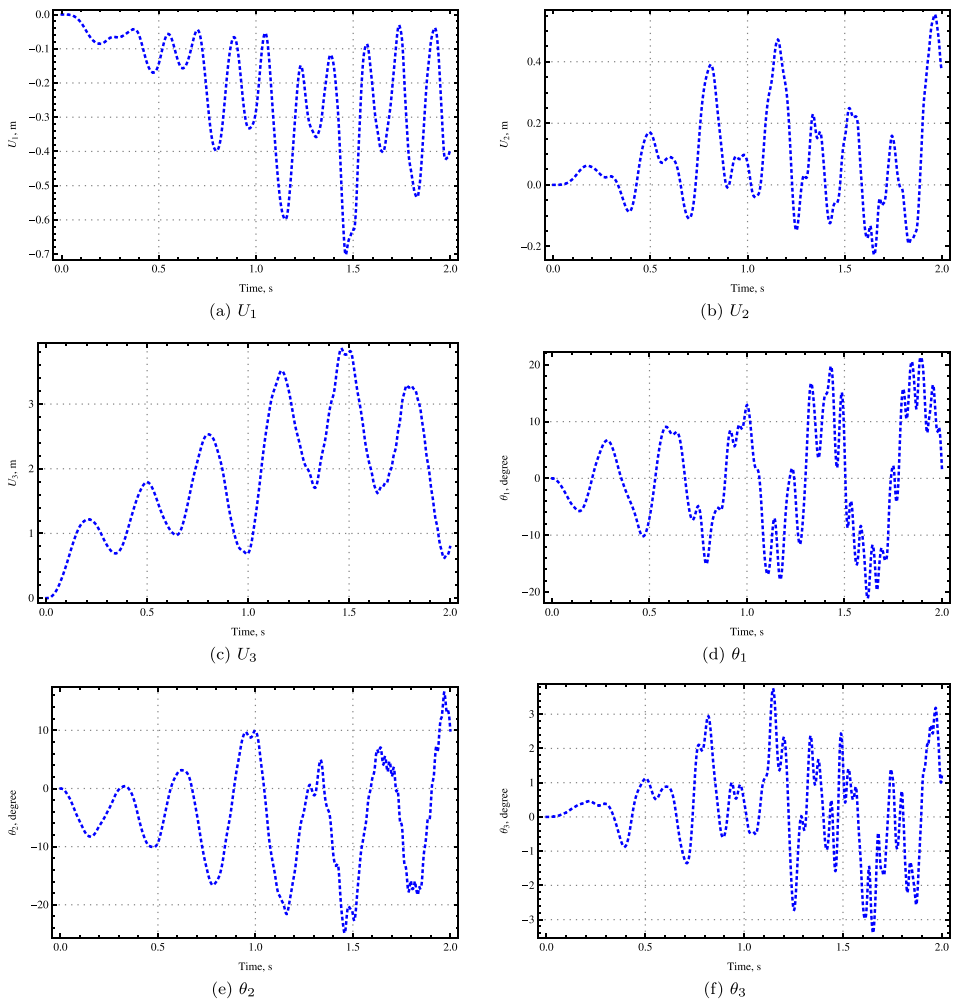

(a) U_1 (b) U_2 (c) U_3 (d) θ_1 (e) θ_2 (f) θ_3

FIG. 10. Tip displacement and rotation histories of a realistic wind turbine blade under a vertical tip load.

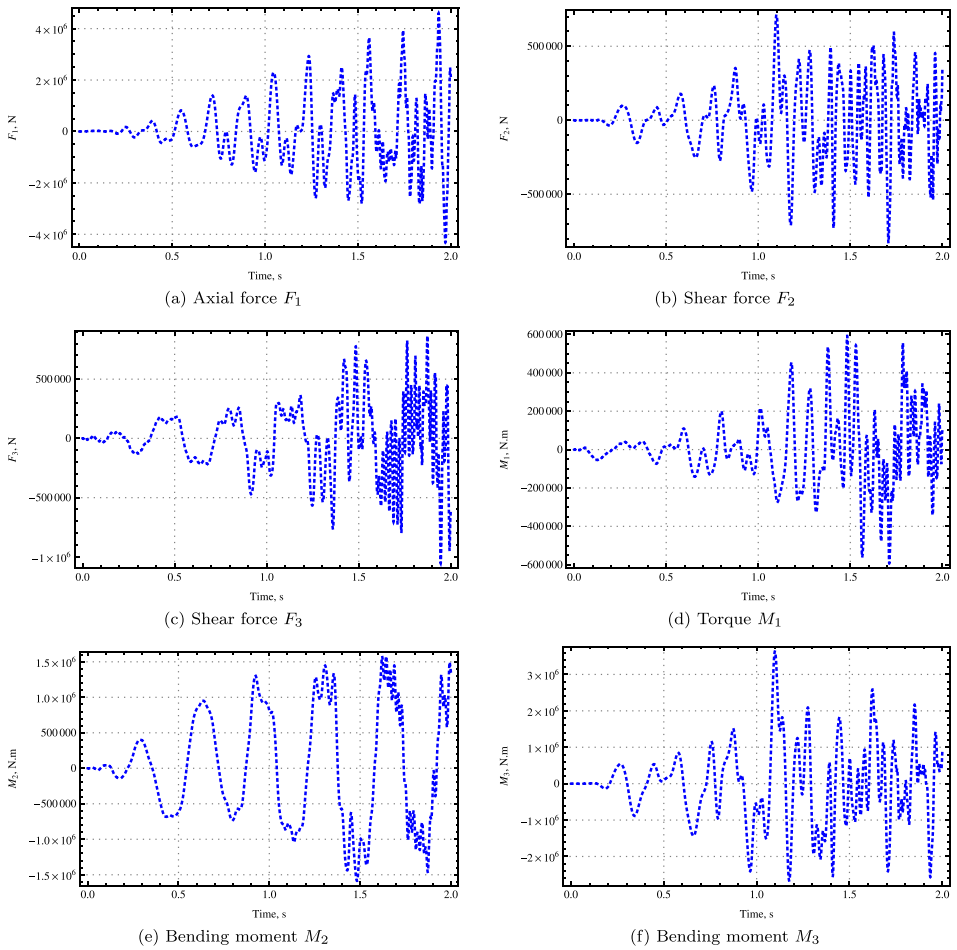

(a) Axial force F_1 (b) Shear force F_2

(c) Shear force F_3 (d) Torque M_1

(e) Bending moment M_2 (f) Bending moment M_3

FIG. 11. Stress-resultant time histories at the root of a wind turbine blade.

beam is divided into 10 elements in the GEBT calculation, and a sinusoidal point force governed by Eq. (57) is applied at the free tip in the z direction with $A_F = 1.0 \times 10^5$ N and $\omega_F = 20$ rad/s (see Fig. 8). A sketch of this example is shown in Fig. 9. The time step used in this example is 0.001 s so that a set of converged results can be achieved. The tip displacement and rotation histories of the beam are plotted in Fig. 10. Note that all the components including three displacements and three rotations are non-zero due to the coupling effects. The time histories of the stress resultants at the root of the beam are given in Fig. 11.

V. CONCLUSION

This paper presents an implementation and validation of the geometrically exact beam theory. Based on previous work,[14] Wiener-Milenković parameters are chosen to describe beam rotations. While the valid range of rotation is extended, there is, however, due to the analytical nature of the mixed formulation, a singularity when the rotation reaches 2π. Given the fact that the kinematics of the present work are implemented in a body-attached coordinate system $\underline{a}_i$, this valid rotation range should be enough for most of the practical design scenarios of wind turbine blades and slender structural parts of other renewable energy systems. Numerical examples are presented that demonstrate the capability of the present beam solver. Two benchmark static problems for geometric nonlinear and curved beams are studied. The agreement between the results calculated by the proposed model and the analytical solution and those available in the literature is excellent. A dynamic analysis of a beam assembly is conducted using GEBT and ANSYS, and GEBT shows a good agreement with ANSYS for displacements and natural

frequencies. Finally, a composite beam with a realistic wind turbine cross-section is analyzed where all coupling effects were accounted for, including those among extension, shear, bending, and torsion. To sum up, GEBT is a powerful tool for composite beam analysis. Its features including large rotation and elastic coupling effects make it especially suitable for the structural design of modern MW-scale composite wind turbine blades.

ACKNOWLEDGMENTS

The authors thank Dr. Michael A. Sprague and Dr. Khanh Nguyen for useful conversations. The authors also thank Professor Oliver A. Bauchau for technical discussions on the 3D rotation parameters.

[1]Q. Wang, W. Yu, and M. A. Sprague, "Geometric nonlinear analysis of composite beams using Wiener-Milenković parameters," in Proceedings of the 54th AIAA/ASME/ASCE/AHS/ASC Structures, Structural Dynamics, and Materials Conference, Boston, Massachusetts (2013).
[2]D. T. Griffith and T. D. Ashwill, "The Sandia 100-meter all-glass baseline wind turbine blade: Snl100-00," Technical Report No. SAND2011-3779, Sandia National Laboratories, 2011.
[3]E. Reissner, "On one-dimensional large-displacement finite-strain beam theory," Stud. Appl. Math. **52**, 87–95 (1973).
[4]D. H. Hodges, *Nonlinear Composite Beam Theory* (AIAA, 2006).
[5]J. C. Simo, "A finite strain beam formulation. the three-dimensional dynamic problem. Part I," Comput. Methods Appl. Mech. Eng. **49**, 55–70 (1985).
[6]J. C. Simo and L. Vu-Quoc, "A three-dimensional finite-strain rod model. Part II," Comput. Methods Appl. Mech. Eng. **58**, 79–116 (1986).
[7]G. Jelenić and M. A. Crisfield, "Geometrically exact 3d beam theory: Implementation of a strain-invariant finite element for statics and dynamics," Comput. Methods Appl. Mech. Eng. **171**, 141–171 (1999).
[8]P. Betsch and P. Steinmann, "Frame-indifferent beam finite elements based upon the geometrically exact beam theory," Int. J. Numer. Methods Eng. **54**, 1775–1788 (2002).
[9]A. Ibrahimbegović, "On finite element implementation of geometrically nonlinear Reissner's beam theory: Three-dimensional curved beam elements," Comput. Methods Appl. Mech. Eng. **122**, 11–26 (1995).
[10]A. Ibrahimbegović, F. Frey, and I. Kožar, "Computational aspects of vector-like parameterization of three-dimensional finite rotations," Int. J. Numer. Methods Eng. **38**, 3653–3673 (1995).
[11]A. Ibrahimbegović and M. A. Mikdad, "Finite rotations in dynamics of beams and implicit time-stepping schemes," Int. J. Numer. Methods Eng. **41**, 781–814 (1998).
[12]F. Auricchio, P. Carotenuto, and A. Reali, "On the geometrically exact beam model: A consistent, effective and simple derivation from three-dimensional finite-elasticity," Int. J. Solids Struct. **45**, 4766–4781 (2008).
[13]R. D. Cook, D. S. Malkus, M. E. Plesha, and R. J. Witt, *Concepts and Applications of Finite Element Analysis*, 4th ed. (Wiley, 2001).
[14]W. Yu and M. Blair, "Gebt: A general-purpose nonlinear analysis tool for composite beams," Compos. Struct. **94**, 2677–2689 (2012).
[15]M. J. Patil, D. H. Hodges, and C. E. S. Cesnik, "Limit-cycle oscillations in high-aspect-ration wings," J. Fluids Struct. **15**, 107–132 (2001).
[16]W. Yu, D. H. Hodges, V. V. Volovoi, and C. E. S. Cesnik, "On Timoshenko-like modeling of initially curved and twisted composite beams," Int. J. Solids Struct. **39**, 5101–5121 (2002).
[17]Q. Wang and W. Yu, "Variational-asymptotic modeling of the thermoelastic behavior of composite beams," Compos. Struct. **93**, 2330–2339 (2011).
[18]J. P. Blasques and M. Stolpe, "Multi-material topology optimization of laminated composite beam cross sections," Compos. Struct. **94**, 3278–3289 (2012).
[19]Y. Li, N. Karri, and Q. Wang, "Three-dimensional numerical analysis on blade response of a vertical-axis tidal current turbine under operational conditions," J. Renewable Sustainable Energy **6**, 043123 (2014).
[20]O. A. Bauchau, *Flexible Multibody Dynamics* (Springer, 2010).
[21]J. Argyris, "An excursion into large rotations," Comput. Methods Appl. Mech. Eng. **32**, 85–155 (1982).
[22]D. Hodges, "A mixed variational formulation based on exact intrinsic equations for dynamics of moving beams," Int. J. Solids Structures **26**, 1253–1273 (1990).
[23]N. Xiao and H. Zhong, "Non-linear quadrature element analysis of planar frames based on geometrically exact beam theory," Int. J. Non-Linear Mech. **47**, 481–488 (2012).
[24]J. M. Mayo, D. García-Vallejo, and J. Domínguez, "Study of the geometric stiffening effect: Comparison of different formulations," Multibody Syst. Dyn. **11**, 321–341 (2004).
[25]K. J. Bathe and S. Bolourchi, "Large displacement analysis of three-dimensional beam structures," Int. J. Numer. Methods Eng. **14**, 961–986 (1979).
[26]W. Su and C. E. Cesnik, "Strain-based geometrically nonlinear beam formulation for modeling very flexible aircraft," Int. J. Solids Struct. **48**, 2349–2360 (2011).
[27]H. Chen, W. Yu, and M. Capellaro, "A critical assessment of computer tools for calculating composite wind turbine blade properties," Wind Energy **13**, 497–516 (2010).